Time-correlation analysis of simulated water motion in flexible and rigid gramicidin channels

See-Wing Chiu,* Eric Jakobsson,*‡ Shankar Subramaniam,§ and J. Andrew McCammon§‖
*Dept. of Physiology and Biophysics, University of Illinois, Urbana, Illinois 61801; ‡Program in Bioengineering, University of Illinois, Urbana, Illinois 61801; §Department of Chemistry and Institute for Molecular Design, University of Houston, Houston, Texas 77204; and ‖Department of Physiology and Molecular Biophysics, Baylor College of Medicine, Houston, Texas 77030 USA

ABSTRACT Molecular dynamics simulations have been done on a system consisting of the polypeptide membrane channel former gramicidin, plus water molecules in the channel and caps of waters at the two ends of the channel. In the absence of explicit simulation of the surrounding membrane, the helical form of the channel was maintained by artificial restraints on the peptide motion. The characteristic time constant of the artificial restraint was varied to assess the effect of the restraints on the channel structure and water motions. Time-correlation analysis was done on the motions of individual channel waters and on the motions of the center of mass of the channel waters. It is found that individual water molecules confined in the channel execute higher frequency motions than bulk water, for all degrees of channel peptide restraint. The center-of-mass motion of the chain of channel waters (which is the motion that is critical for transmembrane transport, due to the mandatory single filing of water in the channel) does not exhibit these higher frequency motions. The mobility of the water chain is dramatically reduced by holding the channel rigid. Thus permeation through the channel is not like flow through a rigid pipe; rather permeation is facilitated by peptide motion. For the looser restraints we used, the mobility of the water chain was not very much affected by the degree of restraint. Depending on which set of experiments is considered, the computed mobility of our water chain in the flexible channel is four to twenty times too high to account for the experimentally measured resistance of the gramicidin channel to water flow. From this result it appears likely that the peptide motions of an actual gramicidin channel embedded in a lipid membrane may be more restrained than in our flexible channel model, and that these restraints may be a significant modulator of channel permeability. For the completely rigid channel model the "trapping" of the water molecules in preferred positions throughout the molecular dynamics run precludes a reasonable assessment of mobility, but it seems to be quite low.

INTRODUCTION

A large number of simulations and other computations have been carried out on models of the Gramicidin A ion channel protein (for recent reviews, see Pullman, 1987; Jordan, 1987, 1988). Owing to the difficulty in modeling lipid membranes and for other reasons of computational tractability, all these computations have been carried out without including explicit representation of the surrounding phospholipid membrane structure. (In recent papers Åqvist and Warshel [1989] and Jordan [1990] included some generalized low dielectric material in part of the region where the membrane would be.) The ion transport through gramicidin A channels is modified by modifications of the lipid environment (Sawyer et al., 1989) and it is reasonable to assume that in addition to interacting chemically, the membrane has the effect of constraining the channel. The influence of such a constraint can be probed theoretically by carrying out simulations under various constraints and the analysis of the transport properties of the channel waters and the ions should reflect this.

In a recent study (Chiu et al., 1989) we investigated, using the techniques of molecular dynamics, the structure and motions of water in the gramicidin A ion channel. The study revealed the existence of conformational substates for the channel waters and we probed the transitions between them. In this paper, we describe the results of our detailed analysis on the nature of the channel waters from time correlation analysis of the dynamics trajectories under a variety of constraints of the channel. The objective of the study is twofold. Firstly, we analyze our results with a view to understand the structure and motions of the channel waters as opposed to bulk waters. Secondly, by applying various constraints which reduce the range of motion of the peptide, we study the influence of such constraints on the water structure and transport. Although these restraints are not an explicit representation of the lipid-peptide interaction, to the extent that the lipid acts by restricting the range of peptide motions, the lipid may modify the channel water structure and motions similarly to the way the artificial restraints do.

The structure of bound waters in biological systems has been an object of considerable attention owing to their structural and functional significance (Wong et al.,

Dr. Subramaniam's present affiliations are Department of Chemistry, Princeton University, Princeton, NJ 08544 and Squibb Institute for Medical Research, Princeton, NJ 08543.

1989). Of special interest to the study of ion channels are questions concerning the nature of channel waters as opposed to bulk water and a comparison of their structural and dynamical properties. Our previous study (Chiu et al., 1989) elaborated on the highly correlated nature of the water structure in the gramicidin channel, initially shown by Mackay et al. (1984). Roux and Karplus (1990), using the CHARMM molecular dynamics program, also find highly correlated water structure. Jordan (1990), using a spherical dipole model for N-H and C-O groups in the peptide backbone and a polarizable water model, sees much less water structure correlation than we and the other workers cited above. In this paper we study the dynamical behavior of the channel waters. We also compare it against the behavior of bulk waters that are used as caps at either end of the channel. The size of the channel caps is enlarged as compared with our previous simulations, and the enlarged size aids in eliminating as end artifacts water correlations in the channel. Also, the runs are longer than in the previous study, to ensure adequate sampling for doing time-correlation analysis on the data. The transport properties of the channel waters are best analyzed through the self-diffusion coefficients, velocity autocorrelation functions (VACF), and the spectral density functions obtained from the VACF's. The latter can also yield the frequencies that reflect the normal modes of collective motion. In the next section we outline briefly the simulation methods and theoretical underpinnings of our analysis of the simulations.

THEORY AND SIMULATION DETAILS

An important quantity for study of dynamical behavior is the long time diffusion rate, which is measured by the self-diffusion coefficient D. The self-diffusion coefficient can be evaluated from the VACF in the following manner (McQuarrie, 1976; Chandler, 1987):

For one-dimensional diffusion (for example, along the axis of an ion channel), the velocity autocorrelation function for a moving particle is given by:

$$\mathrm{VACF}(t) = \langle v(0) \cdot v(t) \rangle. \tag{1}$$

The self-diffusion coefficient then follows from the VACF:

$$D = \int_0^\infty dt \mathrm{VACF}(t). \tag{2}$$

The velocities in the expression for the VACF are those calculated by the molecular dynamics simulations. In this paper we will be concerned with the diffusion of water in the gramicidin channel. For each water molecule, the instantaneous velocity is taken as the center of mass of the three-atom system; i.e., the oxygen and the two hydrogens. In addition to the motion of individual water molecules in the channel and the caps of water just outside the channel, it will be of interest to analyze the motion of the chain of waters inside the channel. It has long been noted that the gramicidin channel is so narrow that ions and water molecules must move through it in a single-file fashion. (For a review of water movement through gramicidin, see Chapter 8 of Finkelstein, 1987.) Therefore the motion of the center-of-mass of the chain of the waters in the channel correlates particularly clearly with the net diffusive motion of water through the channel and across the membrane, because the independent fluctuations of the individual water molecules largely cancel in calculations of this collective property.

Purely diffusive motion is characterized by a molecular relaxation time, which is given by:

$$\tau_{\mathrm{relax}} = mD/kT. \tag{3}$$

In the case of predominantly diffusive motion, the initial and final velocities are expected to be completely decorrelated for time periods longer than the molecular relaxation time. Simulations of bulk fluids display this behavior, both for simple molecules such as argon (Rahman, 1964) and also such complicated molecules as water (Rahman and Stillinger, 1971). Longer time correlations that persist after all the tails are properly accounted for, reveal existence of collective modes of motion that keep the system correlated for longer time scales. In such cases the integral on the right-hand side of Eq. 2 does not converge or converges very slowly, so that Eq. 2 is not useful for calculating the diffusion coefficient. Another instance in which the integral on the right-hand side of Eq. 2 will not yield the effective diffusion coefficient is for diffusion in a periodic potential (Lifson and Jackson, 1962). In those instances an effective diffusion coefficient for one-dimensional motion may be obtained by a mean-square displacement (MSD) correlation according to the following relationship:

$$D = \lim_{t\to\infty}[(x(t) - x(0)^2]/2t. \tag{4}$$

All of the trajectories and correlation functions for water motion computed in this paper were computed relative to r (radial) and z (longitudinal) "channel coordinates," defined as follows: the centers of mass of each monomer of the gramicidin channel are continually monitored. The channel axis ($r = 0$) is defined as the line joining the two centers of monomer mass at each instant. The channel center ($r = 0, z = 0$) is defined as the midpoint of this line at each instant.

For some of the motions the velocity autocorrelation

function is Fourier analyzed and the spectral density function (SDF) computed. For this purpose the SSWD routine of the IMSL statistical library was used. A modified Bartlett window with a parameter of 150 was used.

The simulation method employed in this work is similar to that described in a previous paper (Chiu et al., 1989) and hence only a cursory outline will be provided. Recent NMR and circular dichroism data indicate that the gramicidin A channel helix is right-handed. (Arseniev et al., 1985; Nicholson and Cross, 1989; Andersen et al., 1990) Therefore, the right-handed model structure of gramicidin A analogous to the left-handed model of Koeppe and Kimura (1984) was used as a starting point (Chiu et al., 1990) in the simulations. A point which merits mention here is the use of nonelastic restraints (Chiu et al., 1989) to assess the mobility of the channel waters under varying restraints. This nonelastic restraint is restricted to protein atoms and provides a first order relaxation of each atomic position r toward a reference position r_0, according to the expression:

$$dr/dt = (r_0 - r)/\tau_r. \quad (5)$$

In the above expression τ_r is the relaxation time for each atomic position to relax toward its specified reference position. The effect of this restraint is to maintain the overall shape of the protein but not to have any major obvious influence on the local motions.

The above procedure does not conserve energy. For this reason as well as the well-known tendency for the temperature to drift (usually upwards) in the course of a molecular dynamics simulation, it is necessary to couple the system to a heat bath to maintain a constant temperature. We used the method of Berendsen et al. (1984). In this method all atomic velocities are rescaled at each time step, relaxing back toward the reference temperature with a characteristic relaxation time. For the purpose of calculating the scale factors, the temperatures of the peptide and of the population of waters were calculated independently of each other so that the artificial restraints on the peptide motion wouldn't have a direct effect on the scaling of the water motions. In our simulations the relaxation time was chosen to be 0.2 ps.

To minimize the possibility of boundary-condition-induced artifacts in the computed motions inside the channel, we have increased the number of water molecules in the caps at each end of the channel from 7 to 25. The increased "surface area" of the cap caused "evaporation" of water molecules from the cap; i.e., occasionally a water molecule would break away from the cap. This necessitated one addition to our previous methods to prevent this evaporation. To accomplish this, the water positions were monitored and tested to see if they were either within the channel or within a cube 9 Å on a side with the center of the channel mouth at the center of one of the cube faces. When a water molecule that is outside the channel strays outside of the boundaries of the cube, a restoring motion is imposed on that molecule, restoring it toward the nearest cube face. The form of the motion is with a time constant of 10 ps toward the nearest point on the face of the cube. Note that the water caps themselves will not be cubes because 25 water molecules are not enough to fill a 9 Å cube at normal water density. Thus the cap is a somewhat irregular shape within the cube. The precise shape of the cap and the precise nature of the "anti-evaporation" restraints are not important in this study as long as they do not significantly influence the behavior within the channel. We will show the evidence pertaining to this in Results and Discussion. A visualization of the simulated system is shown in Fig. 1 *A*.

All simulations were carried out at 300°K. The system was heated to 300°K in a similar fashion to our previous paper (Chiu et al., 1989). At 300°K an additional procedure was introduced to let the system generate its own reference coordinates, as opposed to continuing to use the Koeppe-Kimura coordinates throughout the data gathering. The full procedure at 300°K was as follows: conformational data were retained for the first 20 ps at 300°K. In the next 20 ps the mean conformation of the first 20 ps was used as the reference conformation data were retained. At the conclusion of the second 20 ps, the reference coordinates were adjusted to be the average channel conformation during the second 20 ps. The system was then permitted to run for another 20 ps, during which no data were retained. Finally, after this third 20 ps interval at 300°K, data collection was begun, and the same reference conformation was used for the remainder of the run, which was an additional 240 ps. The above procedure was first done with a restraint relaxation time of 20 ps. Additional MD simulations were performed with restraint relaxation times of 40 and 60 ps. For the runs with 40- and 60-ps restraint relaxation times, the mean structure determined with the 20-ps restraint relaxation time was used as the original reference structure, rather than using the Koeppe-Kimura structure. The mean conformations of the peptide were not significantly different for different relaxation times. Simulations were also done for the channel peptide held rigid. In this instance the above method for determining the conformation could not be used since the peptide conformation obviously could never deviate from the original Koeppe-Kimura helix. For the rigid-channel calculations the conformation determined for the 20 ps relaxation time was used. The water temperature in the rigid-channel computations was 300°K but the channel temperature was 5°K. All simulations were

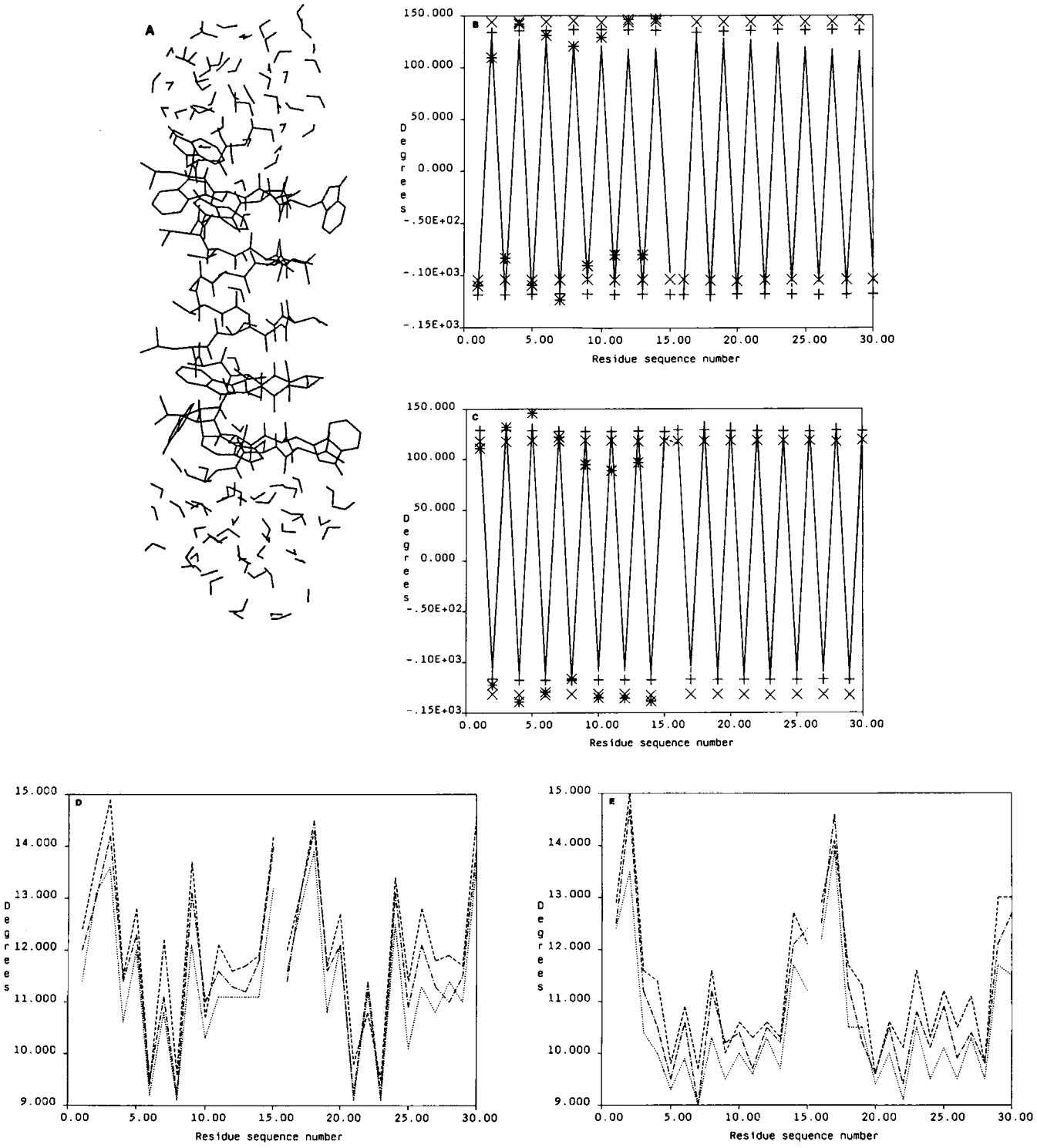

FIGURE 1 (*A*) The simulated molecular system, including the gramicidin A dimer with waters in the channel and caps of water contained in cubic regions at the ends of the channel. (*B*) Backbone ϕ angles for our MD-produced structure as compared with other structures. This figure was produced with lines coded according to degrees of soft constraint as follows: rigid channel is solid line, 20 ps is dotted line, 40 ps is dot-dash line, 60 ps is dashed line. In *A* and *B* separate lines are mostly not separately visible because they lie on top of each other. Other symbols: +, Koeppe-Kimura; x, Venkatachalam-Urry (1984) model; *, Urry model after energy minimization (Roux and Karplus, 1988). Our model is right-handed, all other models transposed to right-handed versions. Residues numbered 1–15 from channel center to channel mouth for one monomer, 16–30 for the other monomer. (*C*) Same as *B* for ψ angles, (*D*) RMS deviation from mean value during 240 ps MD run at 300°K of ϕ angles. (*E*) Same as *D* for ψ angles.

done on the Cray 2 computer at the National Center for Supercomputing Applications.

The choice of using Koeppe-Kimura coordinates as the starting structure as opposed to the Venkatachalam-Urry (1984) coordinates is to a certain extent arbitrary, but we do have some basis for choosing Koeppe-Kimura. When we did energy minimization using the right-handed versions of both as a starting point, we found the structure derived from Koeppe-Kimura to have significantly lower energy than that derived from Venkatachalam-Urry. It may be that how the tryptophan rings are stacked is a more significant difference between the Venkatachalam-Urry and the Koeppe-Kimura configurations than the backbone structures. (Side-chain orientations are not reported in the Koeppe-Kimura paper, but Dr. Koeppe shared their assumed orientations with us in a personal communication.) We have done high-temperature (400 K) dynamics with only the backbone restrained (Brenneman et al., 1991). When we start with the side chains in the Venkatachalam-Urry configuration we find that after 40 ps at 400°K, the tryptophan rings have flipped over to the type of stacking suggested by Koeppe and Kimura. For these reasons we prefer the Koeppe-Kimura structure as the starting reference structure for building our structure. It should be emphasized that the final structure is a new structure, not that of either Venkatachalam and Urry or Koeppe and Kimura. It is a right-handed helix, whereas both Venkatachalam-Urry and Koeppe-Kimura are left-handed. It is produced by time average configurations produced by molecular dynamics computations, which is quite different from the process by which either Venkatachalam-Urry or Koeppe-Kimura were produced. We previously noted (Chiu et al., 1989) that in our MD-produced structure there was a systematic tendency for the C-O bonds to bend in to the lumen of the channel, in contrast to both the Venkatachalam-Urry and the Koeppe-Kimura structures.

Another measure of the deviation of our structure from those idealized ones is the dihedral angles of the backbone, which are shown in Figs. 1, *B* and *C*, and compared Koeppe-Kimura, Venkatachalam-Urry, and the result of energy minimizing the Urry structure as reported in Roux and Karplus (1988). The Koeppe-Kimura and Venkatachalam-Urry structures are of course quite regular. Our MD-produced structure is much more regular than the energy-minimized Urry structure. Roux and Karplus (1988) ascribed the irregularity of the energy-minimized Urry structure to the finite length of the helix and side chain interference. Because our relatively regular structure is derived from a finite helix, these results suggest that the major reason for the irregularity of the energy-minimized Urry helix is strain transmitted to the backbone by side chain interference.

Although the mean structures are essentially identical for all degrees of restraint of our flexible channel models, the range of motion is greater the less extreme the restraint, just as would be expected. We demonstrate this in Figs. 1, *D* and *E*, where we show the RMS deviation of the backbone dihedral angles. There is some tendency for the angles associated with the *D*-amino acids to show more fluctuation than the L-amino acids. There is a pronounced tendency for the ends of each monomer to show larger fluctuations from the mean structure than does the central region of each monomer. This is possibly due to the larger number of intramonomer hydrogen bonds per linkage in the central regions.

RESULTS AND DISCUSSION

Fig. 2 shows water molecular trajectories and dipole orientations during the course of the MD simulations carried out in this study. These data differ from those presented in our previous study (Chiu et al., 1989) in having much longer runs and also in exploring various degrees of channel flexibility. It should be noted that the trajectories and orientations shown are for all water molecules that spent any part of the MD runs in the channel; some of the molecules shown spent part of the run outside the channel. The striking feature of the rigid channel computations is that the water molecules definitely have preferred positions (Fig. 2 *A*) and the water molecule dipoles remain similarly oriented throughout the duration of the run (Fig. 2 *E*). From the flexible channel trajectories (Figs. 2 *B–D*) it appears that the same water positions are preferred as for the rigid channels but that a higher mobility is achieved by virtue of more frequent shifts of the water chain from one position to another. In the flexible as in the rigid channels there is a tendency for the water dipoles to align in the same direction as each other (Figs. 2 *F–H*). However, in the flexible channels there are clearly larger fluctuations from that alignment. Some individual water molecules in the flexible channels break away from the overall alignment for extended periods of time and on three separate occasions (twice in the 20-ps run and once in the 40-ps run) the dipole moment of the entire chain of waters flips in a coordinated way.

The results of Fig. 2 on water–water dipole alignment are consistent with molecular dynamics results of Mackay et al. (1984) and Roux and Karplus (1990) but not those of Jordan (1990). Jordan's results show much less correlation of channel water dipole orientation and much more frequent reversals of individual water dipole

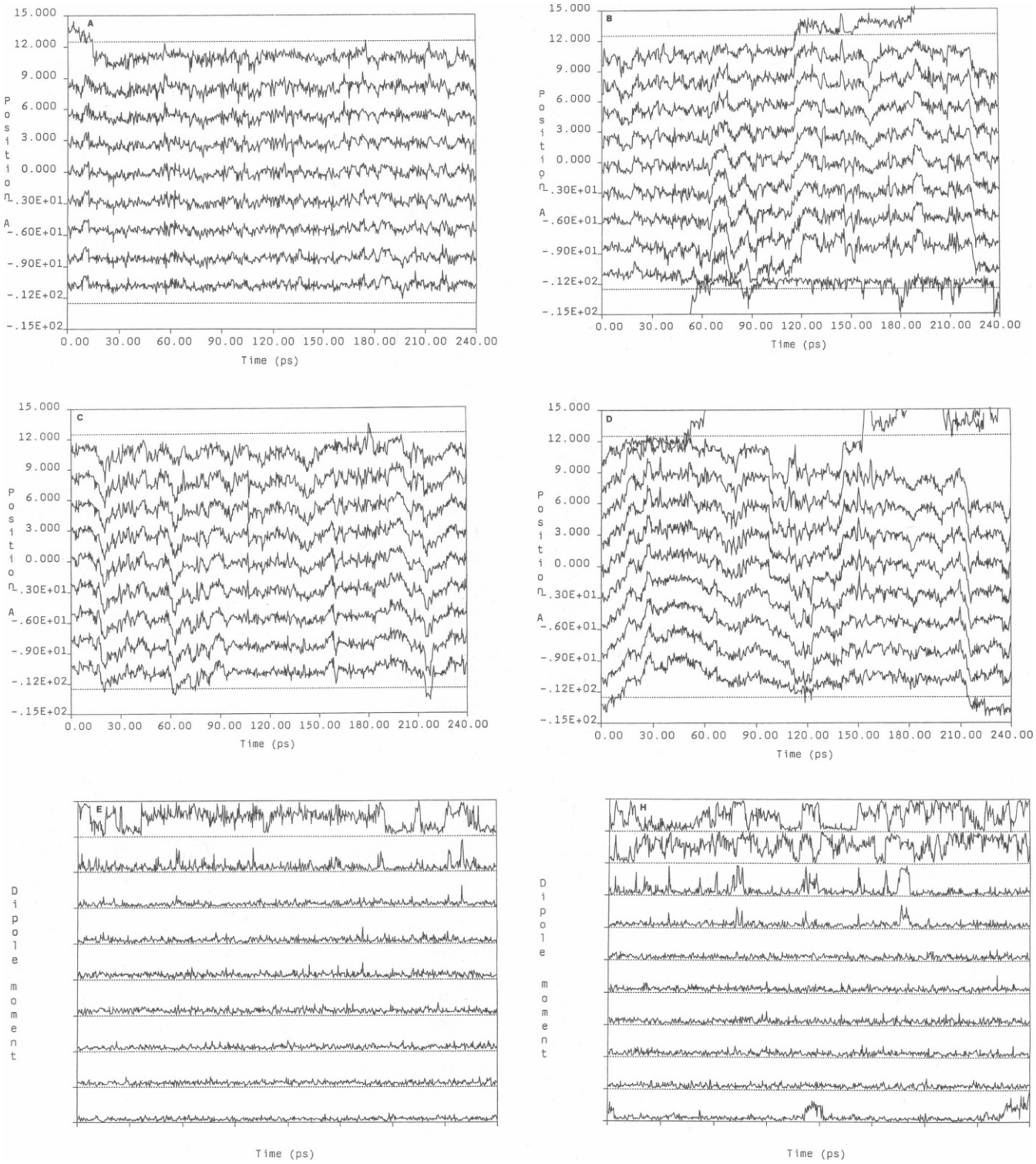

FIGURE 2 Raw data for 240 ps molecular dynamics runs at 300°K with various degrees of all-atom restraints on the peptide motions. (*A–D*) Trajectories of individual channel water molecules in the direction along the channel axis. (*A*) Rigid channel, (*B*) 20 ps time constant, (*C*) 40 ps time constant, (*D*) 60 ps time constant. (*E–H*) Projections of water dipole moments on the long axis of the channel for various degrees of all-atom restraints on the peptide motions. Dotted lines indicate condition where water dipole moment is precisely parallel to the long axis of channel. (*E*) rigid channel, (*F*) 20 ps time constant.

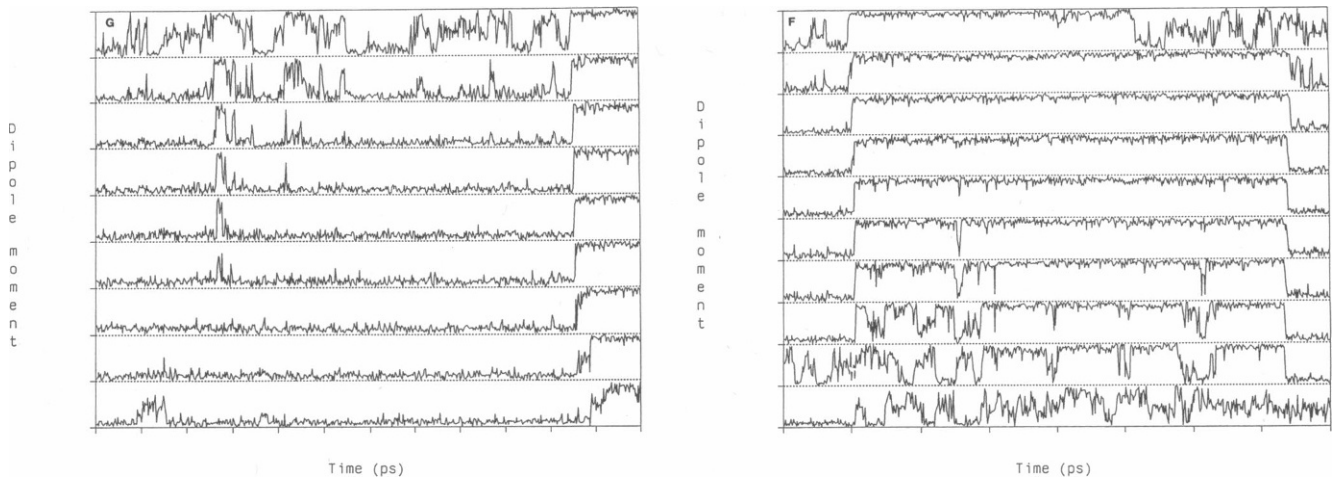

FIGURE 2 (continued) (*G*) 40 ps time constant, (*H*) 60 ps time constant.

orientation than other workers. His model differs from others in two significant respects. One is that he uses a polarizable water model. The second is that he uses a reduced model of the channel backbone in which the N-H and C-O are Lennard-Jones spheres with no point charges but rather with a point dipole in the center. We think it unlikely that the polarizable water is the cause of the qualitatively different behavior because polarizability ordinarily *increases* net attraction between molecules and their tendency to have systematic orientations relative to each other. Thus the polarizability would seem likely to change the system behavior in the opposite direction from that seen in Jordan's paper. A more likely reason for the difference lies in Jordan's dipole approximation for the channel backbone. In the full channel model the carbonyl oxygens tend to tilt in toward the channel lumen, facilitating the formation of hydrogen bonds with the water hydrogens (Chiu et al., 1989). These hydrogen bonds restrain the water motions, both translational and rotational. In Jordan's reduced backbone model there is no explicit carbonyl oxygen charge, so this aspect of peptide-water interaction is absent. We interpret Jordan's results as implying that if one removes the ability of the peptide to make hydrogen bonds with the waters, the water barriers to rotation of water molecules are reduced. This reduction would explain the absence of preferred orientations.

In this paper we carry out time-correlation analysis on the motions of the system in such a manner as to reveal the ways in which the motion of channel waters is similar to, and different from, the motion of water in bulk solution. It is important to verify whether our waters in the "caps" outside the ends of the ion channel behave similarly to bulk waters. Figs. 3, *A* and *B*, show the normalized velocity autocorrelation function (VACF) and the spectral density function (SDF) of the VACF for the cap waters. (The normalized VACF is just the VACF divided by the mean square velocity. All of the VACF's presented in this paper are normalized.) Because our system has some geometrical anisotropy, the VACF is shown for each of the three Cartesian coordinates, with the *z*-coordinate oriented along the long axis of the channel. It is seen that these curves are very similar, essentially identical, to those computed for SPC water in bulk using periodic boundary conditions (Berendsen et al., 1984). Because of this similarity we believe that our boundary conditions are not likely to introduce spurious or artifactual features into our observed correlation functions for water inside the channel, even though our system lacks the symmetry that would make periodic boundary conditions feasible. We also looked for "transition" waters; i.e., water molecules that are in the cap region but remain very near the mouth of the channel. It is conceivable that there might be a class of water molecules that would have properties intermediate between the channel waters and those farther out in the bulk. But we found no such class of water molecules. Instead we found that waters near the channel mouth were as mobile as those farther out in the cap, and also that there was no tendency for waters to remain near the channel mouth as long as they were actually outside the channel; i.e., more than ~13–13.5 Å from the center of the channel. Thus there seem to be just two definable classes of water molecules, channel and bulk, an important caveat here being that the calculated system did not include the phospholipid system around the mouth of

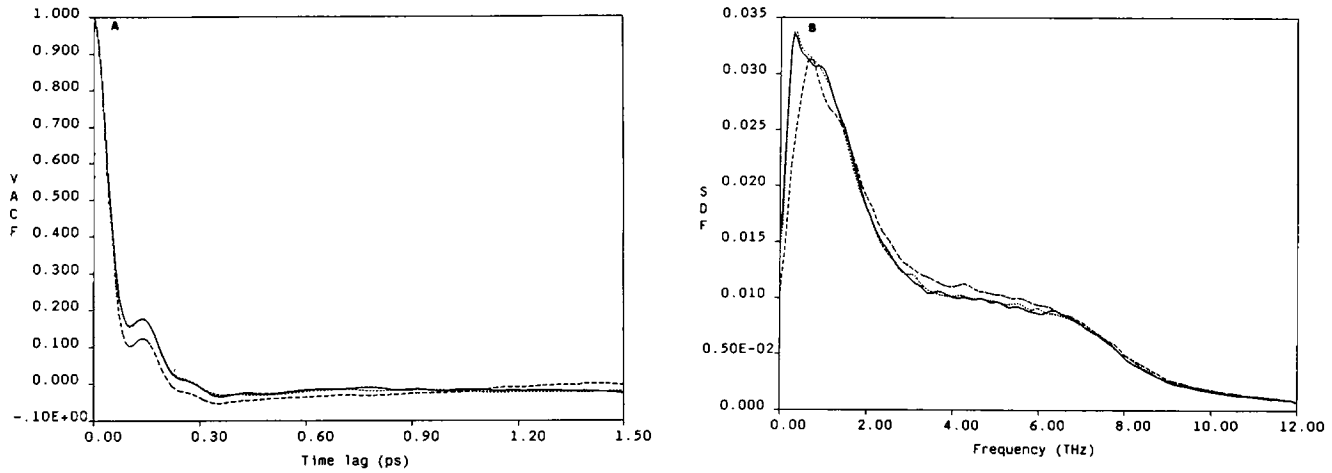

FIGURE 3 Spectral properties of cap water motions. To verify isotropy, motions are correlated in x (*solid line*), y (*dotted line*), and z (*dashed line*) directions. (*A*) Normalized velocity autocorrelation function (VACF) for the individual waters in the cap. This figure is very similar to the corresponding figure for bulk water calculated using periodic boundary conditions. (Berendsen et al., 1984). (*B*) Spectral density function (SDF) of the VACF in Fig. 3 *a*. This figure is very similar to the corresponding figure for bulk water calculated using periodic boundary conditions (Berendsen et al. 1984).

the channel. From previous studies (Lee et al., 1984; Egberts and Berendsen, 1988) it appears that the waters adjacent to the membrane surface near the mouth of the channel would be nonrandomly oriented and have different dynamics from bulk water. Thus a more complete simulation with the explicit lipid layers would be more revealing.

In contrast to the water molecules in the cap, the channel waters exhibit behavior very different from bulk water. Figs. 4, *A* and *B*, display the mean normalized VACF and the average SDF along the z-axis (long axis of the channel) averaged over all the individual channel waters. As is apparent from the the contrast with Figs. 3, *A* and *B*, the high frequency components of motion are much more dominant for the waters within the channel. The calculations are shown for several different values of τ_r, the restraint time constant for the channel peptide. The loosest restraint is 60 ps, and the tightest restraint, 0.01 ps, essentially yields a completely rigid channel. It is seen that the spectral properties of the subpicosecond fluctuations of individual water molecules seem relatively unaffected by the extent of the peptide motion.

In contrast to bulk water, the motion in the channel is anisotropic. Therefore we display the normalized VACF and corresponding SDF for radial motion (motion of the waters normal to the long axis of the channel) in Figs. 4, *C* and *D*. It is seen that the radial motion is relatively monotonic and lacks many of the higher frequency components of the motion along the channel axis. Like the motion along the channel axis, the spectral properties of the radial motions of the individual waters are not much affected by the extent of the peptide motion. However, there does seem to be a bit more oscillatory character to the VACF for the rigid channel than for the flexible channel models. The motion of the water in the rigid channel has more of the characteristics of oscillations in a periodic lattice than does the motion in the flexible channel.

The narrow dimensions of the gramicidin channel mandate single-file water motion because it is almost impossible for one water to pass another within the channel. Furthermore, molecular dynamics studies of water motion in the channel show that the motions of the waters are highly correlated (Mackay et al., 1984; Mackay and Wilson, 1986; Chiu et al., 1989; Roux and Karplus, 1990; Jordan, 1990). Thus the chain of waters in the channel moves in some ways similar to a single particle, and it is just this type of coordinated movement that is the critical determinant of the rate of net water transport through the channels. We show the mean-square-deviation (MSD, Eq. 4) of the center of mass movement along the channel axis in Fig. 5, for various degrees of restraint of polypeptide motion. One outstanding feature of Fig. 5 is that the water center-of-mass motion along the channel axis is not purely Brownian but rather seems partially restrained in potential wells. This can be seen by the bending over of the MSD function. The relative free energy minima are reflected in the preferred positions seen in the trajectories of Fig. 2. For very short correlation times the motion is relatively free. The initial slope of the MSD function near the origin gives the fluid dynamic diffusion coefficient for the motion of the chain of waters, according to

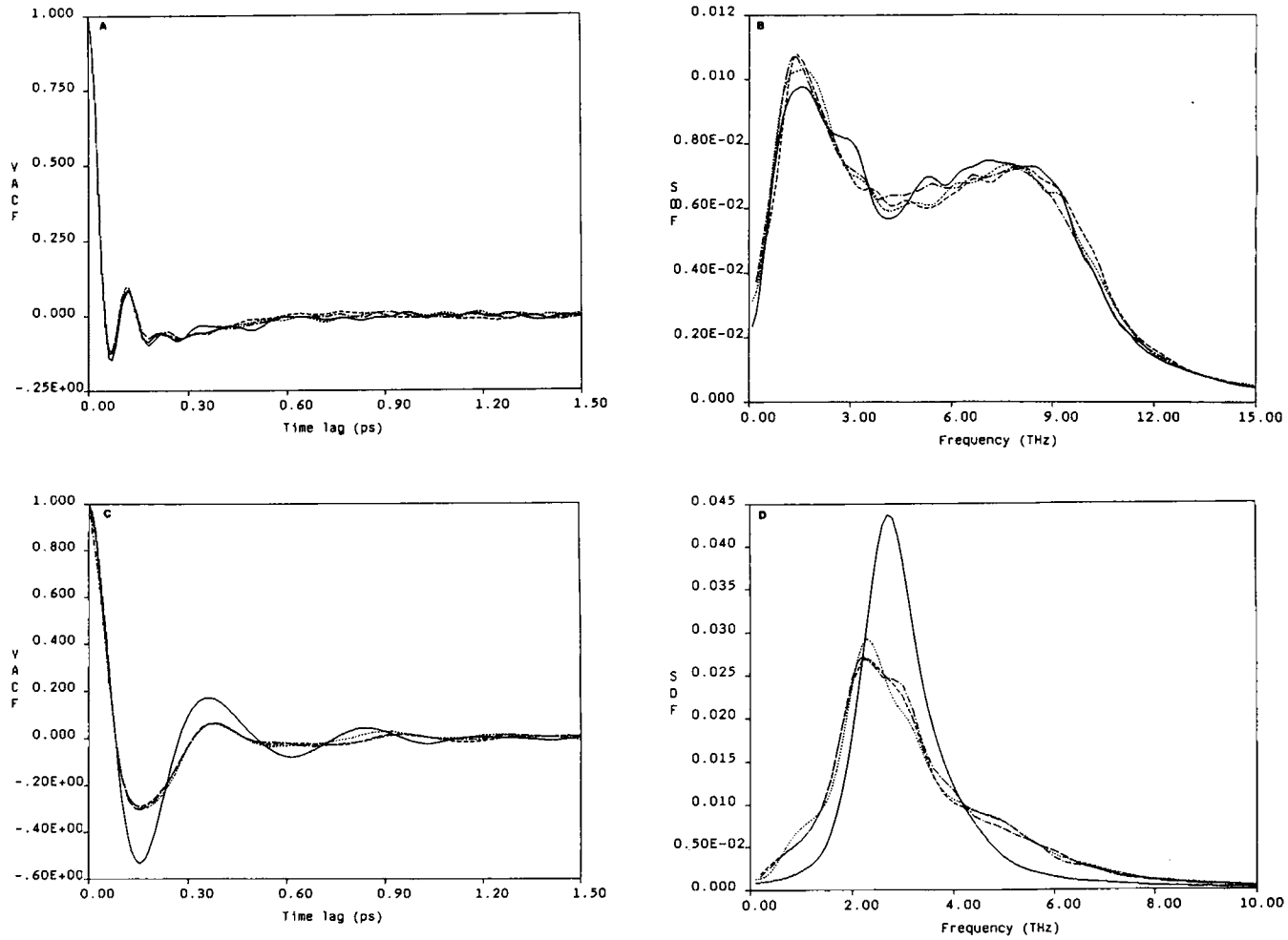

FIGURE 4 Spectral properties of individual channel water motions for various degrees of peptide restraint. (Solid line is rigid channel; dotted line is $\tau_r = 20$ ps; dot-dash line is $\tau_r = 40$ ps; dashed line is $\tau_r = 60$ ps.) (*A*) Normalized velocity autocorrelation function (VACF) for individual channel waters in the *z* direction for each of the all-atom restraint runs, (*B*) spectral density function (SDF) of *A*. Note that compared with cap waters the channel waters exhibit much more high-frequency motion, and that the spectrum is essentially identical for the rigid and flexible channel models. (*C*) VACF for individual channel waters in the radial direction for each of the all-atom restraint runs, (*D*) SDF of *C*. Note that the radial motions tend to be more monochromatic than the longitudinal motions, and that the dominant frequency is significantly higher than the dominant frequency for cap water motions. The SDF is somewhat more monochromatic for the rigid channel than for the flexible channel models.

the relationship $D = (\Delta X^2)/(2 \times \Delta t)$. Farther from the origin, the final slope of the MSD function gives the effective diffusion coefficient for translation of the chain of waters across the channel. It is seen that the fluid dynamic diffusion coefficient is not a very strong function of degree of peptide motion. For all degrees of peptide restraint, the fluid dynamic diffusion coefficient is $\sim 1.8 \times 10^{-5}$ cm^2/s. This is quite close to the self-diffusion coefficient of bulk water. Thus it appears that the fluid dynamic friction for the chain of waters in the channel when the waters are in preferred positions in local energy minima is similar to the hydrodynamic friction in bulk water. On the other hand, the effective diffusion coefficient for translocation of waters across the channel depends on the peptide motion. For the runs in which the peptide motion is only loosely restrained the effective diffusion coefficient is substantially more than for the rigid channel. The heights of the free energy barriers for water translocation seem substantially higher for the rigid channel.

Some aspects of these motions can be illuminated by analyzing components of water motion normal to the channel axis. Fig. 6*A* shows the MSD of the center of mass of the water chain in the radial direction normal to the axis of the channel as a function of degree of restraint on the polypeptide. This figure shows that the

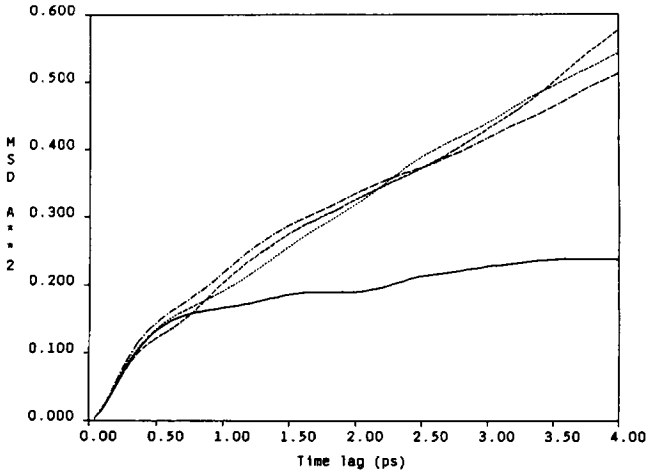

FIGURE 5 Mean square deviation or MSD ($\langle z(t)^2 - z(0)^2 \rangle$) correlation function of center of mass of chain of waters along channel axis for each of the all-atom restraints. (solid line is rigid channel; dotted line is τ_r = 20 ps; dot-dash line is τ_r = 40 ps; dashed line is τ_r = 60 ps.) Note that the effective diffusion coefficient is substantially higher for the flexible channel models than for the rigid channel model.

range of radial motion is significantly greater for the flexible channels than for the rigid channel. Note also in Fig. 6, *A* and *B*, the pronounced oscillatory motions of water in the rigid channel, as was noted in Fig. 4 *C*. Fig. 6 *B* shows the VACF for the center of mass motion of the water chain in the radial direction. Comparison of Figs. 6 *B* and 4 *C* reveal a striking similarity between the VACF's for radial motion of the chain of waters and individual waters. This similarity implies that for radial motions, the chain of waters moves as a unit. Fig. 6 *C*, the SDF of Fig. 6 *B*, provides further evidence for this collective movement when compared with Fig. 4 *D*, the corresponding SDF for individual water radial movement. The frequencies for motion of the water chain and the individual waters are very similar.

The normalized VACF and corresponding SDF for the motion of the water chain center of mass along the channel axis are shown in Figs. 7, *A* and *B*. Compared with the corresponding curves for the average individual channel water, relatively lower frequency components are dominant. Frequency components much higher than 1–2 THz are noticeably absent. Only the lowest fre-

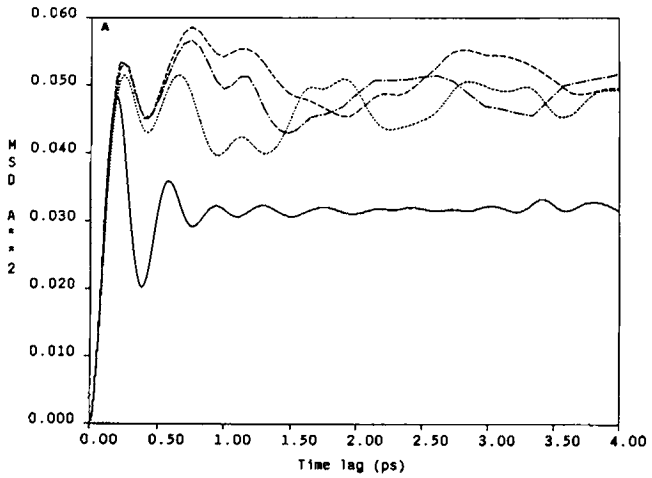

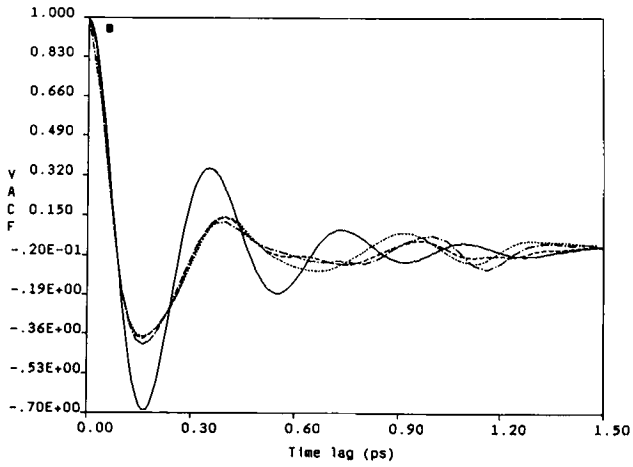

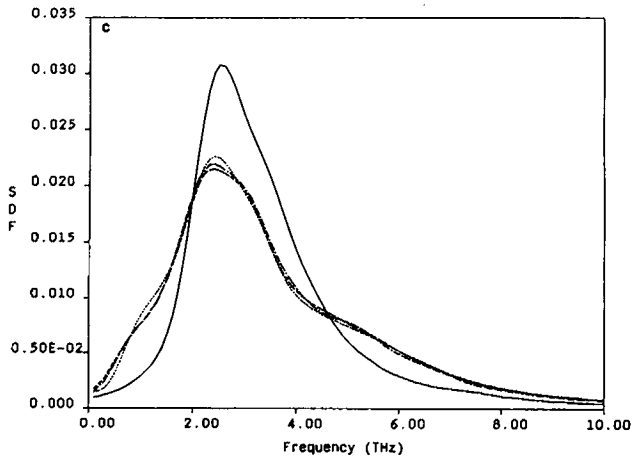

FIGURE 6 Radial fluctuations of the center-of-mass of the water chain. Solid curves are rigid channel; dotted curves are τ_r = 20 ps; dot-dash curves are τ_r = 40 ps; dashed curves are τ_r = 60 ps. (*A*) Mean squared deviation (MSD) correlation of radial center-of-mass motions of the water chain for each of the all-atom restraints. Note that the amplitude of the collective radial water motions is significantly lower in the rigid channel than in the flexible channel models. (*B*) Normalized VACF for radial motion of the center of mass of the water chain. (*C*) Spectral density funciton (SDF) of *a*. Note similarity between SDF for collective radial motions normal to the channel axis (this figure) and the corresponding SDF for collective longitudinal motions parallel to the channel axis (Fig. 4 *D*).

quency component of the individual channel water motions is identifiable with the motion of the entire chain of waters. The contrast between the VACF's of the center of mass of the water chain (Fig. 7 *A*) and of the individual channel waters (Fig. 4 *A*) highlights the correlated nature of the waters in the channel. There is no major systematic shift in the dominant frequency of the motion of the chain waters along the channel axis (Fig. 7 *B*) with the degree of restraint of the channel peptide motions. Interestingly, the dominant frequencies in the center of mass motions of the chain of channel waters (Figs. 6 *A* and 7 *B*) are always of the same order of magnitude as the dominant frequency of the motions of *individual* waters in bulk (Fig. 3 *B*). They also happen to be of the same order as the sonic resonance frequency of a column of water the length of a gramicidin channel, calculated by dividing the velocity of sound in water by the channel length. We do not know at this time which of these correspondences, if either, actually explains the frequency of the collective water motion in the channel.

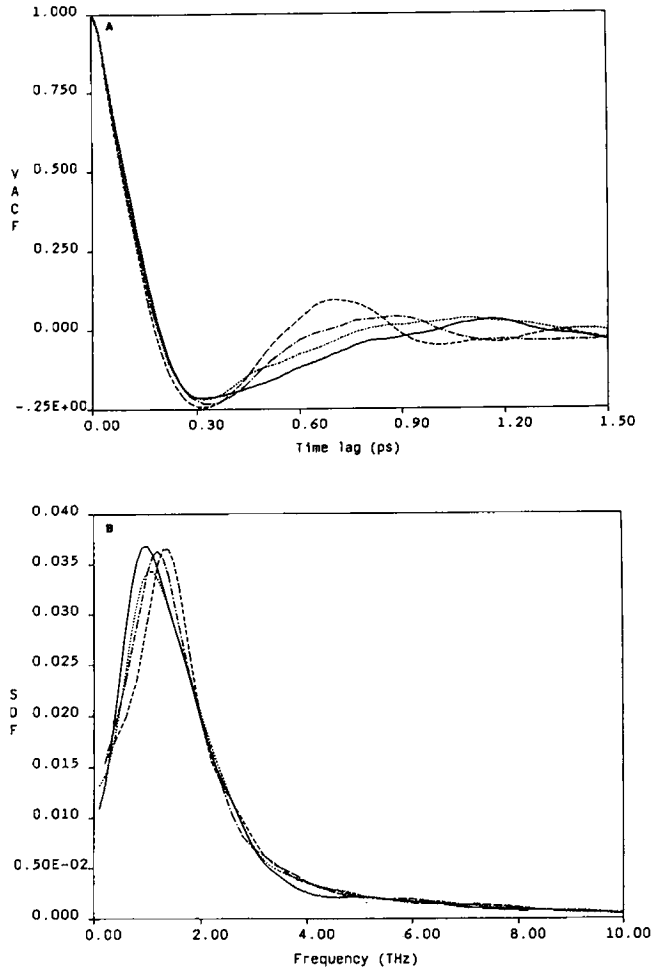

FIGURE 7 Spectral properties of center-of-mass water motion along the axis. Solid curves are rigid channel; dotted curves are τ_r = 20 ps; dot-dash curves are τ_r = 40 ps; dashed curves are τ_r = 60 ps. (*A*) Velocity autocorrelation function (VACF) for center-of-mass of the chain of waters for each of the all-atom restraints. (*B*) Spectral density function (SDF) for *A*. (*B*) shows that the dominant frequency of the collective water motion along the channel axis is not a strong function of the degree to which the peptide motions are restrained, and is closer to bulk water than to individual channel water molecules.

The above data show clearly the dominant source of the high frequency components of the water motion inside the channel. One might hypothesize them to come from one of two sources: (*a*) the existence of many higher frequency normal modes for the gramicidin channel (Naik and Krim, 1986; Roux and Karplus, 1988), or (*b*) the confinement of waters within the peptide. Because we see the high-frequency components strongly present when the channel motion is restrained tightly (including being made completely rigid), it is clear that it is primarily the confinement in the channel rather than the imposition of the high-frequency normal modes of the channel polypeptide that gives rise to the high-frequency components of the channel water motion.

Dynamical behavior of a simulated system is reflected in the diffusion behavior. It is of interest to infer the diffusion coefficient from the short time fluctuations. Two measures of the diffusion coefficient are: (*a*) the zero-frequency intercept of the SDF curve, and (*b*) the slope of the MSD curve. For channel waters the situation is more complicated than for bulk water and other liquids, due to the preferred positions for the water molecules. In this case the effective diffusion coefficient is given by twice the slope of the curves in Fig. 5 at long time lags after they have bent over. For the flexible channel models, the value calculated from Fig. 5 is 6×10^{-6} cm^2/s. For the rigid channel model the slope is not meaningfully different from zero, because for the entire run the water molecules only fluctuated around one set of preferred positions. All that can be said with confidence is that the effective diffusion coefficient is much less for the rigid channel model than for the flexible channel models. Dani and Levitt (1981), using experimental values for the hydraulic permeability coefficient, calculated a diffusion coefficient for the water chain of 1.7×10^{-6} cm^2/s. The same analysis applied to the data of Rosenberg and Finkelstein (1978) results in a value of 2.8×10^{-7} cm^2/s. Our value of diffusion coefficient for the flexible channel model is substantially higher than either of these values. This suggests that the membrane lipid (which we do not explicitly simulate) may provide significant restraint on channel motion, which in turn reduces the water mobility in the channel. It should also be noted that the SPC water model we use has a

self-diffusion coefficient in bulk 1.8 times as large as the experimental value (Berendsen et al., 1987).

SUMMARY AND CONCLUSIONS

Several novel features of water transport through gramicidin-like ion channels emerge from our simulations and analysis.

Firstly, the most significant result is the long-range sustained correlations amongst channel waters and a confirmation of previous results that the diffusion along the channel axis involved a collective coordinate. We find that the MSD correlation function for motion along this coordinate bends over as one might expect for thermally driven motion in the presence of periodic barriers.

Secondly, this paper systematically analyzes the role of varying channel restraints on the water motions and transport. Making the channel rigid reduces the amplitude of the collective water motions in the radial direction and reduces the mobility of the water chain along the long axis of the channel. Relaxation of constraints on the protein channel seems to reduce the height of the free energy barriers to the motion of the water chain along the channel axis, as indicated by the form of the MSD correlation. Further stochastic simulations of such a system (Jakobsson and Chiu, 1988; Chiu and Jakobsson, 1990) may throw more light on the kinetic properties.

Experience with other simulations of peptides and proteins suggests that our model of the gramicidin channel combined with SPC water should provide a reasonable representation of this system. The motion of water confined in a gramicidin channel deviates more from a purely Brownian diffusive model than does that of water in bulk. One obvious difference is that all net motions are one-dimensional, along the long axis of the channel. The VACF for individual channel water molecules in the longitudinal direction shows a distribution of higher frequency components than are seen for bulk water at 300°K. The individual channel water VACF is somewhat similar to that which has been reported for supercooled water in bulk (Stillinger and Rahman, 1972). The channel water motion that is most significant for transport is the center-of-mass of the chain of channel waters because of the obligatory single-filing of water in the channel. The spectral density for this motion is similar to that for bulk water, but the VACF shows a much more pronounced undershoot than for bulk water and also shows an overshoot absent in the VACF for bulk water. Finally the MSD for channel water shows a bending over that is absent in the MSD for Brownian particles or bulk water, indicating periodic free energy barriers to water translocation in the channel. In this sense the water motion in the channel is similar to ion diffusion in a polyelectrolyte solution (Lifson and Jackson, 1962).

At Illinois, this work was supported by National Institutes of Health grant PHS RO1GM32356 to Dr. Jakobsson. At Houston, this work was supported in part by the National Science Foundation and the Robert A. Welch Foundation via grants to Dr. McCammon. Dr. McCammon is the recipient of the George Herbert Hitchings Award from the Burroughs Wellcome Fund. Grants of computer time from the National Center for Supercomputing Applications at Illinois were received by both Dr. Jakobsson and Dr. McCammon.

Received for publication 17 May 1990 and in final form 8 February 1991.

REFERENCES

Andersen, O. S., L. L. Providence, and R. E. Koeppe II. 1990. Gramicidin channels are right-handed β-helical dimers. *Biophys. J.* 57:100*a*. (Abstr.)

Åqvist, J., and A. Warshel. 1989. Energetics of ion permeation through membrane channels. Solvation of Na^+ by gramicidin A. *Biophys. J.* 56:171–182.

Arseniev, A. S., I. L. Barsukov, V. F. Bystrov, A. L. Lomize, and A. Yu. Ovchinnikov. 1985. ^{1}H-NMR study of gramicidin A transmembrane ion channel. Head-to-head right-handed, single-stranded helices. *FEBS (Fed. Eur. Biochem. Soc.) Lett.* 186:168–174.

Berendsen, H. J. C., J. P. M. Postma, W. F. van Gunsteren, A. DiNola, and J. R. Haak. 1984. Molecular dynamics with coupling to an external bath. *J. Chem. Phys.* 81:3684–3690.

Berendsen, H. J. C., J. R. Grigera, and T. P. Straatsma. 1987. The missing term in effective pair potentials. *J. Phys. Chem.* 91:6269–6271.

Brenneman, M., S.-W. Chiu, and E. Jakobsson. 1991. Computational studies on the side chain conformations of gramicidin A. *Biophys. Soc. Annu. Meet. Abstr.*

Chandler, D. 1987. Introduction to Modern Statistical Mechanics. Oxford University Press, Oxford. 234–270.

Chiu, S. W., and E. Jakobsson. 1990. Molecular dynamics analysis of ion movements in the gramicidin channel. *Proc. 10th Intl. Biophys. Cong.* 1:392.

Chiu, S. W., S. Subramaniam, E. Jakobsson, and J. A. McCammon. 1989. Water and polypeptide conformations in the gramicidin channel. A molecular dynamics study. *Biophys. J.* 56:253–261.

Chiu, S. W., L. Nicholson, M. T. Brenneman, S. Subramaniam, Q. Teng, C. North, J. A. McCammon, and E. Jakobsson. 1990. Molecular dynamics computations and solid state NMR of the gramicidin cation channel. *Biophys. J.* 57:101*a*. (Abstr.)

Dani, J. A. and D. G. Levitt. 1981. Water transport and ion-water interactions in the gramicidin channel. *Biophys. J.* 35:501–508.

Egberts, E., and H. J. C. Berendsen. 1988. Molecular dynamics simulation of a smectic liquid crystal and atomic detail. *J. Chem. Phys.* 89:3718–3732.

Finkelstein, A. 1987. Water Movement through Lipid Bilayers, Pores, and Plasma Membranes. Wiley-Interscience, New York. 130–151.

Hermans, J., H. J. C. Berendsen, W. F. van Gunsteren, and J. P. M. Postma. 1984. A consistent empirical potential for water-protein interactions. *Biopolymers.* 23:1513–1518.

Jakobsson, E., and S. W. Chiu. 1988. Application of Brownian motion theory to the analysis of membrane channel ionic trajectories calculated by molecular dynamics. *Biophys. J.* 54:751–756.

Jordan, P. C. 1987. Microscopic approaches to ion transport through transmembrane channels. The model system gramicidin. *J. Phys. Chem.* 91:6582–6591.

Jordan, P. C. 1988. Ion transport through transmembrane channels: Ab initio perspectives. *Curr. Top. Membr. Transp.* 33:91–111.

Jordan, P. C. 1990. Ion-water and ion-polypeptide correlatins in a gramicidin-like channel. A molecular dynamics study. *Biophys. J.* 58:1133–1156.

Koeppe, R. E. II, and M. Kimura. 1984. Computer building of β-helical polypeptide models. *Biopolymers.* 23:23–38.

Lee, C. Y., J. A. McCammon, and P. J. Rossky. 1984. The structure of liquid water at an extended hydrophobic surface. *J. Chem. Phys.* 80:4448–4455.

Lifson, S., and J. L. Jackson. 1962. On the self-diffusion of ions in a polyelectrolyte solution. *J. Chem. Phys.* 36:2410–2414.

Mackay, D. J. H., and K. R. Wilson. 1986. Possible allosteric significance of water structures in proteins. *J. Biomol. Struct. & Dyn.* 4:491–500.

Mackay, D. J. H., J. Berens, K. R. Wilson, and A. T. Hagler. 1984. Structure and dynamics of ion transport through gramicidin A. *Biophys. J.* 46:229–248.

McQuarrie, D. A. 1976. Statistical Mechanics. Harper and Row, New York. 452–542.

Naik, V. M., and S. Krimm. 1986. Vibrational analysis of the structure of gramicidin A. I. Normal mode analysis. *Biophys. J.* 49:1131–1145.

Nicholson, L. K., and T. A. Cross. 1989. The gramicidin cation channel: an experimental determination of the right-handed helix sense and verification of β-type hydrogen bonding. *Biochemistry.* 28:9379–9385.

Pullman, A. 1987. Energy profiles in the gramicidin A channel. *Q. Rev. Biophys.* 20,3/4:173–200.

Rahman, A. 1964. Correlations in the motion of atoms in liquid argon. *Phys. Rev. A.* 136:405–411.

Rahman, A., and F. Stillinger. 1971. Molecular dynamics study of liquid water. *J. Chem. Phys.* 55:3336–3359.

Rosenberg, P. A., and A. Finkelstein. 1978. Water permeability of gramicidin A-treated lipid bilayer membranes. *J. Gen. Physiol.* 72:341–350.

Roux, B., and M. Karplus. 1988. The normal modes of the gramicidin A dimer channel. *Biophys. J.* 53:297–309.

Roux, B., and M. Karplus. 1990. Theoretical study of ion transport in the gramicidin A channel. *Proc. 10th Int. Biophys. Congr. (Vancouver).* 391.

Sawyer, D. B., R. E. Koeppe, II, and O. S. Andersen. 1989. Induction of conductance heterogeneity in gramicidin channels. *Biochemistry.* 28:6571–6583.

Stillinger, F. H., and A. Rahman. 1972. Molecular dynamics study of temperature effects on water structure and kinetics. *J. Chem. Phys.* 57:1281–1292.

Venkatachalam, C. M., and D. W. Urry. 1984. Theoretical conformational analysis of the gramicidin A transmembrane channel. I. Helix sense and energetics of head-to-head dimerization. *J. Comput. Chem.* 4:461–469.

Wong, C. F., J. Shen, C. Zheng, S. Subramaniam, and J. A. McCammon. 1989. Molecular dynamics of protein hydration. *J. Mol. Liq.* 41:193–206.